Distinctive properties and expression profiles of glutamine synthetase from a plant symbiotic fungus

Barbara MONTANINI*, Marco BETTI†, Antonio J. MÁRQUEZ†, Raffaella BALESTRINI‡, Paola BONFANTE‡ and Simone OTTONELLO*[1]

*Dipartimento di Biochimica e Biologia Molecolare, Università di Parma, Parco Area delle Scienze 23/A, I-43100 Parma, Italy, †Departamento de Bioquímica Vegetal y Biología Molecular, Facultad de Química, Universidad de Sevilla, Apartado 553, E-41080-Sevilla, Spain, and ‡Istituto per la Protezione delle Piante, Sezione di Micologia del Terreno, CNR, Dipartimento di Biologia Vegetale, Università di Torino, Viale Mattioli 25, I-10125 Torino, Italy

Nitrogen retrieval and assimilation by symbiotic ectomycorrhizal fungi is thought to play a central role in the mutualistic interaction between these organisms and their plant hosts. Here we report on the molecular characterization of the key N-assimilation enzyme glutamine synthetase from the mycorrhizal ascomycete *Tuber borchii* (TbGS). TbGS displayed a strong positive co-operativity ($n = 1.7 \pm 0.29$) and an unusually high $S_{0.5}$ value (54 ± 16 mM; $S_{0.5}$ is the substrate concentration value at which $v = \frac{1}{2}V_{max}$) for glutamate, and a correspondingly low sensitivity towards inhibition by the glutamate analogue herbicide phosphinothricin. The TbGS mRNA, which is encoded by a single-copy gene in the *Tuber* genome, was up-regulated in N-starved mycelia and returned to basal levels upon resupplementation of various forms of N, the most effective of which was nitrate. Both responses were accompanied by parallel variations of TbGS protein amount and glutamine synthetase activity, thus indicating that TbGS levels are primarily controlled at the pre-translational level. As revealed by a comparative analysis of the TbGS mRNA and of the mRNAs for the metabolically related enzymes glutamate dehydrogenase and glutamate synthase, TbGS is not only the sole messenger that positively responds to N starvation, but also the most abundant under N-limiting conditions. A similar, but even more discriminating expression pattern, with practically undetectable glutamate dehydrogenase mRNA levels, was observed in fruitbodies. The TbGS mRNA was also found to be expressed in symbiosis-engaged hyphae, with distinctively higher hybridization signals in hyphae that were penetrating among and within root cells.

Key words: ammonium assimilation, gene expression, glutamate dehydrogenase, glutamate synthase, glutamine synthetase, mycorrhizal fungi.

INTRODUCTION

Nitrogen is one of the nutrients that most commonly limit plant growth. Accordingly, various strategies have been developed by both plants and soil micro-organisms to increase their N-acquisition capacity. Eco-physiological studies have demonstrated the important contribution of plant-colonizing fungi to the N nutrition of their host plants [1]. Through the formation of specialized symbiotic structures, called ectomycorrhizae, mycorrhizal fungi dramatically expand the effective surface area for nutrient soil exploration, broaden the range of exploitable inorganic and organic N sources, and improve competition with other soil micro-organisms [2]. Central to this mutualistic interaction is the exchange of plant-derived carbohydrates with ready-to-use organic nitrogen sources provided by the fungus [3]. The primary products of inorganic nitrogen assimilation by ectomycorrhizal fungi are glutamate and glutamine [4]. The latter is synthesized by glutamine synthetase (GS; L-glutamate:ammonia ligase, ADP-forming; EC 6.3.1.2), the only amide synthetase capable of incorporating ammonium into the γ-carboxyl of glutamate following ATP-dependent activation. GS plays a central role in N metabolism because it links inorganic N internalization, as well as metabolic processes leading to glutamate, 2-oxoglutarate and ammonium, to N assimilation into protein, nucleic acids and a variety of other N-containing compounds [5]. The incorporation of ammonia into amino acid or ketoacid precursors can occur through the combined action of GS and NADH-dependent glutamate synthase (GOGAT; EC 1.4.1.13) or through the reductive amination of 2-oxoglutarate by NADP-dependent glutamate dehydrogenase (GDH; EC 1.4.1.4) followed by GS-catalysed amidation of glutamate to yield glutamine. The former pathway represents the main route of NH_4^+ assimilation in the roots and photosynthetic tissues of higher plants [6]. A substantial species-specific variability in the preferential utilization of either the GS/GOGAT or the GDH/GS pathway has been reported, instead, for different free-living ectomycorrhizal fungi and plant/fungus associations [4].

Besides being a central biosynthetic precursor and N storage compound, glutamine has been implicated in various microbial systems as a key effector of nitrogen catabolite repression, a regulatory circuit that ensures the preferential utilization of simple N sources (e.g. NH_3) over more complex and expensive ones (e.g. purines, most amino acids and proteins) when multiple N resources are available [7]. Accordingly, GS levels and activity in various fungal systems are finely regulated so to maintain intracellular glutamine concentrations that optimally sustain biosynthesis without resulting in repression or energy-consuming futile cycles. Three main regulatory mechanisms, namely, N-status-dependent biosynthetic modulation (repression/derepression), glutamine-mediated

Abbreviations used: GS, glutamine synthetase; TbGS, *Tuber borchii* GS; rTbGS, recombinant TbGS; GDH, NADP-dependent glutamate dehydrogenase; TbGDH, *Tuber borchii* GDH; GOGAT, NADH-dependent glutamate synthase; TbGOGAT, *Tuber borchii* GOGAT; SSM, synthetic solid medium; EST, expressed sequenced tag; MSX, L-methionine sulphoximine; PPT, L-phosphinothricin.

[1] To whom correspondence should be addressed (e-mail s.ottonello@unipr.it).

The nucleotide sequences reported in this paper have been submitted to the GenBank®/EBI Nucleotide Sequence Databases with accession numbers AF462037 (glutamine synthetase) and AF462032 (glutamate synthase).

enzyme inactivation and GS proteolysis following persistent N starvation have been documented in yeast and other unicellular or multicellular model fungi [7–9]. All of these mechanisms, or subsets of them, may apply to the different life-cycle stages (vegetative, symbiotic and reproductive) of ectomycorrhizal fungi. In fact, besides its general involvement in basal N assimilation as in free-living mycelia, glutamine biosynthesis may play additional, phase-specific roles in more specialized stages of the fungus life-cycle such as mycorrhizae and fruitbodies. For example, GS transcripts have recently been found to be particularly abundant in the fruitbodies of the ectomycorrhizal ascomycete *Tuber borchii* [10], where GS activity is thought to contribute to the synthesis of osmotically active glutamine derivatives as well as to the maintenance, within spore-bearing structures, of adequately low concentrations of the potentially toxic ammonium ion [11]. Similar considerations hold for the mycorrhizal stage, which is known to be favoured by N-limiting growth conditions and negatively influenced by a surplus of nitrogen [3], and where glutamine is thought to be one of the major forms of N transferred from the fungus to the plant [1].

Despite the multiple roles of glutamine in N metabolism and the importance of a well-balanced N status for the correct functioning of the mycorrhizal symbiosis, there are as yet no reports on the molecular characterization of GS throughout the different life-cycle stages of ectomycorrhizal fungi and little is known about the functional properties and N status-dependent regulation of GS in such organisms. Here we report on the isolation of the GS-encoding cDNA from an ectomycorrhizal fungus, the ascomycetous truffle *T. borchii*, the functional characterization of the recombinant GS enzyme and the expression profiling of the corresponding mRNA in free-living mycelia, mycorrhizae and fruitbodies.

MATERIALS AND METHODS

Biological materials

T. borchii Vittad. mycelium (isolate ATCC 95640) was grown in the dark at 23 °C on a synthetic solid medium (SSM), either complete or deprived of a single nutrient, as described previously [12]. In a typical nitrogen-deprivation experiment, mycelia were first grown for 21 days on SSM and then transferred for various lengths of time to either the same medium (mock-shift control, MSC) or to a modified SSM (−N) in which $(NH_4)_2HPO_4$ was replaced by K_2HPO_4. For nitrogen-refeeding experiments, N-starved mycelia were returned for various lengths of time (as specified in the text) to modified SSMs containing NH_4Cl, KNO_3, L-glutamine or L-proline (each at 4 mM) as single N sources. Mycelia utilized for *in situ* hybridization analysis were grown for 30 days in modified Melin–Norkrans liquid nutrient solution (pH 6.6). *T. borchii* fruitbodies (80 % mature) were collected in Piedmont (Italy) and were evaluated for their degree of maturation as described previously [13]. *In vitro*-produced linden (*Tilia platyphyllos*)/*T. borchii* mycorrhizae [14] were provided kindly by D. Sisti (Istituto Botanico, University of Urbino, Urbino, Italy). Mycorrhizal rootlets, at different stages of development, were sampled under a stereomicroscope prior to *in situ* hybridization analysis (see below).

Isolation and sequence analysis of the *Tuber borchii* GS (TbGS) cDNA

A cDNA library constructed in the excisable phage vector Uni-Zap XR from 20-day-old *T. borchii* mycelia (a gift from B. Lazzari and A. Viotti, Istituto di Biologia e Biotecnologia Agraria, CNR, Milan, Italy) was used as a source of template DNA (100 ng/reaction) for PCR amplifications. The oligonucleotides 5′-GGTCCTTACTACTGTGGTGTTGG-3′ (plus) and 5′-CCGGCACCGTTCCAGTCACC-3′ (minus), were utilized for initial amplification experiments that were carried out under previously described 'touchdown' PCR conditions [12], with annealing temperatures ranging from 60 to 50 °C. A cDNA fragment of the expected size (237 bp), 83 % identical in sequence to the *Schizosaccharomyces pombe* GS, was obtained from such amplification and was cloned into the pGEM-T-easy vector (Promega) to generate plasmid pGEM-*TbGS_237*. This cDNA fragment was found subsequently to be identical in sequence to a plasmid-borne cDNA insert (pBlueScript-*TbGS*) picked randomly from the same library in the course of an expressed-sequenced-tag (EST) screening [10].

Sequence-similarity searches were conducted with BLAST on the non-redundant protein database at the National Center for Biotechnology Information (NCBI). Predicted polypeptide sequences were aligned with CLUSTALX. Phylogenetic trees were constructed with the neighbour-joining algorithm implemented in CLUSTALX, and were visualized with the TreeView program.

DNA and RNA analyses

Genomic DNA samples for gel-blot analysis (2 μg each) were digested with *Bam*HI, *Eco*RI and *Hin*dIII, and electrophoresed on 0.8 % agarose gels. Blotting on to GeneScreen Plus (PerkinElmer-Life Science), pre-hybridization and washing were conducted according to the manufacturer's instructions. A random-priming labelling kit (Amersham Biosciences) was used for ^{32}P-labelling of a TbGS cDNA fragment, derived from plasmid pGEM-*TbGS_237*, that was utilized as a probe for DNA and RNA hybridizations. Total RNA for RNA gel-blot and RNase-protection analyses was isolated and quantified as described previously [13]. Heat-denatured total RNA (20 μg for each sample), fractionated on formaldehyde-agarose gels, transferred on to a GeneScreen Plus membrane and hybridized with a ^{32}P-labelled probe derived from the pGEM-*TbGS_237* plasmid, was utilized for high-stringency RNA gel-blot analysis. A *Bgl*II/*Fok*I cDNA fragment derived from plasmid pGEM-*TbGS_237* was subcloned into pBueScript-KS, linearized with *Xba*I, and utilized as a T3 RNA polymerase template to synthesize a TbGS antisense riboprobe (230 nt; final specific activity 15 μCi/pmol) for RNase-protection assays. The *Tuber borchii* GOGAT (TbGOGAT) antisense riboprobe (280 nt; final specific activity 27 μCi/pmol) was prepared by T7 RNA polymerase transcription of a *Bam*HI-linearized TbGOGAT cDNA fragment (accession no. AF462032) isolated previously by homologous PCR and cloned into the pGEM-T-Easy vector. A *T. borchii* GDH (TbGDH) cDNA fragment [15], isolated by homologous PCR and cloned into the pGEM-T-easy vector, was linearized by *Tth*111I digestion and *in vitro*-transcribed with T7 RNA polymerase to prepare the TbGDH antisense riboprobe (276 nt; final specific activity 19 μCi/pmol). Saturating amounts of a β-tubulin riboprobe (259 nt; final specific activity 14.4 μCi/pmol), prepared by T7 RNA polymerase transcription of a *T. borchii* β-tubulin cDNA fragment (354 bp; accession no. AF462033), were added to all reactions as an internal standard. Hybridization (5 μg of total RNA/assay), RNase A/T1 digestion and gel fractionation were carried out as described in [13]. Protected fragments were visualized by autoradiography and quantified with a Personal Imager FX using the Multi-Analyst/PC software (Bio-Rad).

Heterologous expression, purification and analysis of TbGS

The TbGS coding sequence was PCR-amplified (25 cycles) with a proofreading DNA polymerase (*Pfu*; Stratagene) using 10 ng of the pBlueScript-*TbGS* plasmid as a template and the following oligonucleotides (one of which contained an *Nde*I site, underlined) as primers: GS5*Nde* (plus), 5′-TCCATATGAG-CGAAAACTCTAC-3′, and GSpET (minus), 5′-ATCTAAATA-CCACCACAAATCG-3′.

After sequence verification, the product of this amplification reaction was cloned into pGEM-T-Easy, digested with *Nde*I, and transferred into the expression vector pET28b (Novagen). The resulting construct (pET-*TbGS*) was transformed into BL21(DE3) Star *Escherichia coli* cells (Invitrogen). Protein expression was induced by adding 1 mM isopropyl β-D-thiogalactoside and allowed to proceed for 48 h at 20 °C. After cell lysis, recombinant TbGS (rTbGS), bearing an N-terminal hexahistidine tag, was bound to a metal affinity resin (Talon; Clontech) equilibrated in 10 % glycerol/300 mM NaCl/25 mM Tris/HCl pH 8.0, and purified as described in [16]. rTbGS fractions with a purity higher than 90 % (as judged by PAGE analysis, see below) were pooled, dialysed against buffer A (25 mM Tris/HCl, pH 8.0, 0.1 M NaCl, 10 mM $MgCl_2$, 5 mM β-mercaptoethanol and 10 % glycerol) and stored at − 80 °C. Protein concentration was determined with the Coomassie Brilliant Blue G-250 dye method (Bio-Rad) or by UV absorbance using an estimated A_{280} molar absorption coefficient of 63 920 $M^{-1} \cdot cm^{-1}$. The composition and purity of protein fractions were assessed by gel electrophoresis on SDS/PAGE (11 % gel) [17]. Monoclonal antibodies specifically recognizing the N-terminal hexahistidine tag (Amersham Biosciences) were utilized initially for immunoblot analysis of recombinant TbGS following the manufacturer's instructions. Rabbit polyclonal anti-TbGS antibodies and the corresponding pre-immune serum (Eurogentec) were utilized subsequently for the immunodetection of TbGS in electrophoretically fractionated mycelial extracts. To this end, balanced amounts of crude soluble extracts (derived from mycelia subjected to different N regimens, as specified in the text) were electrotransferred to Hybond-ECL (Amersham Biosciences) and analysed with standard procedures using horseradish peroxidase-conjugated anti-rabbit immunoglobulin antibodies and enhanced chemiluminescence reagents (Pierce) according to the manufacturers' instructions. Parallel reactions carried out with the preimmune serum were used as specificity controls.

For gel-filtration analysis, 0.5 ml aliquots of affinity-purified rTbGS (10 mg/ml in buffer A) were run at a flow rate of 0.2 ml/min on a Superdex 200 HR 10/30 column (Amersham Biosciences) equilibrated in 25 mM Tris/HCl (pH 7.5)/0.15 M NaCl. A calibration curve constructed with a set of marker proteins ranging from 13 to 660 kDa (cytochrome *c*, BSA, catalase and thyroglobulin) was used to determine the native molecular mass of rTbGS. Native gel electrophoresis was conducted on 4–15 % PAGE gradients as described in [18], using the HMW Native Marker Kit (Amersham Biosciences) for molecular-mass calibration.

Enzyme assays

The 'biosynthetic reaction' was used for GS assays conducted on the recombinant enzyme as described previously [19,20]:

$$\text{L-Glutamate} + \text{ATP} + NH_4^+ \xrightarrow{Mg^{2+}} \text{L-glutamine} + \text{ADP} + P_i + H^+$$

The standard reaction mixture (final volume 100 μl) contained 10 μmol of Tris/HCl (pH 7.50 at 25 °C), 200 μmol of L-glutamate, 5 μmol of NH_4Cl, 5 μmol of $MgCl_2$, 0.3 μmol of ATP (from a 100 mM stock solution, pH 7.5) and 100–300 ng of affinity-purified rTbGS, dialysed extensively against 10 mM Tris/HCl (pH 7.5)/10 mM $MgCl_2$. Following incubation at 37 °C under linear time-response conditions (up to 60 min), inorganic phosphate released by ATP hydrolysis was determined using the malachite green method [21]. A series of preliminary activity assays conducted at different pH values (4.0–11.0) was run to determine the pH optimum of rTbGS. The kinetic parameters for the different substrates and cofactors were determined by varying the concentrations of individual reaction components (L-Glu, 1–500 mM; NH_4Cl, 0.1–50 mM; ATP, 0.025–10 mM; $MgCl_2$, 0.1–50 mM) in the presence of excess amounts of all the other components. Each enzyme-activity assay was replicated independently at least three times; assays were always conducted in duplicate using parallel reaction mixtures lacking rTbGS as blanks. Data were fitted to a Hanes–Woolf plot ([S]/*v* versus [S]) or to a double-logarithmic Hill plot; regression analysis of the data was performed with SigmaPlot (SPSS). A hexahistidine-tagged derivative of GS from *Phaseolus vulgaris* [19] was purified to near homogeneity by metal affinity chromatography with a procedure similar to the one utilized for rTbGS.

GS activity levels in mycelia subjected to different N regimens (as specified in the text) were determined by the transferase reaction assay [20] using soluble mycelial extracts as a source of enzyme. Extracts were prepared by grinding liquid-N_2-frozen mycelia (100 mg wet weight) suspended in 200 μl of extraction buffer (200 mM Tris/acetate, pH 7.4/2 mM dithiothreitol), followed by centrifugation at 20 000 ***g*** for 10 min (4 °C) and by the determination of the protein content of the resulting supernatants by the Coomassie Brilliant Blue G-250 dye method. Transferase activity assays were conducted at 35 °C under linear time-response conditions (30–120 min) in 0.75 ml reaction mixtures containing 120 mM Mops/NaOH buffer (pH 7.0), 90 mM L-glutamine, 2.4 mM $MnCl_2$, 0.5 mM ADP, 120 mM NH_3OH, 60 mM NaOH, 2 mM dithiothreitol, 50 mM Na_2HAsO_4 plus 20 μg (total protein) of mycelial extracts as a source of enzyme. After the addition of 0.25 ml of blocking reagent (0.4 M $FeCl_3$/3.85 % trichloroacetic acid/0.86 % HCl) and centrifugation at 20 000 ***g*** for 2 min (4 °C), formation of γ-glutamyl hydroxamate was quantified by measuring the absorbance at 500 nm (molar absorption coefficient, 1.08 $M^{-1} \cdot cm^{-1}$). Parallel reaction mixtures from which Na_2HAsO_4 had been omitted were used as blanks.

In situ hybridization analysis

Mycelium and ectomycorrhiza samples were fixed, dehydrated, embedded in paraffin wax, sliced and transferred to poly-L-lysine-pretreated slides as described previously [13]. Sense and antisense digoxygenin-labelled riboprobes for *in situ* hybridization analysis were prepared by *in vitro* transcription (RNA Labelling Kit; Boehringer Mannheim), in reaction mixtures containing digoxygenin-UTP and 1 μg of a linearized plasmid template bearing vector-supplied Sp6 and T7 phage RNA polymerase promoters. *In vitro*-transcription reactions were programmed with linearized (pGEM-T) plasmids carrying either a 273-bp TbGS cDNA fragment cloned in an antisense orientation behind the T7 promoter (pGEM-*TbGS_237*), or a 351-bp fragment of the 18 S rDNA cloned in an antisense orientation behind the Sp6 promoter.

Prior to hybridization, tissue sections were deproteinized and dehydrated following a procedure described previously [13]. Colour development was carried out as described in [22]. The colour reaction was stopped by washing in distilled water. Sections were finally dehydrated through an ethanol/xylene series and mounted in Histovitrex (Carlo Erba).

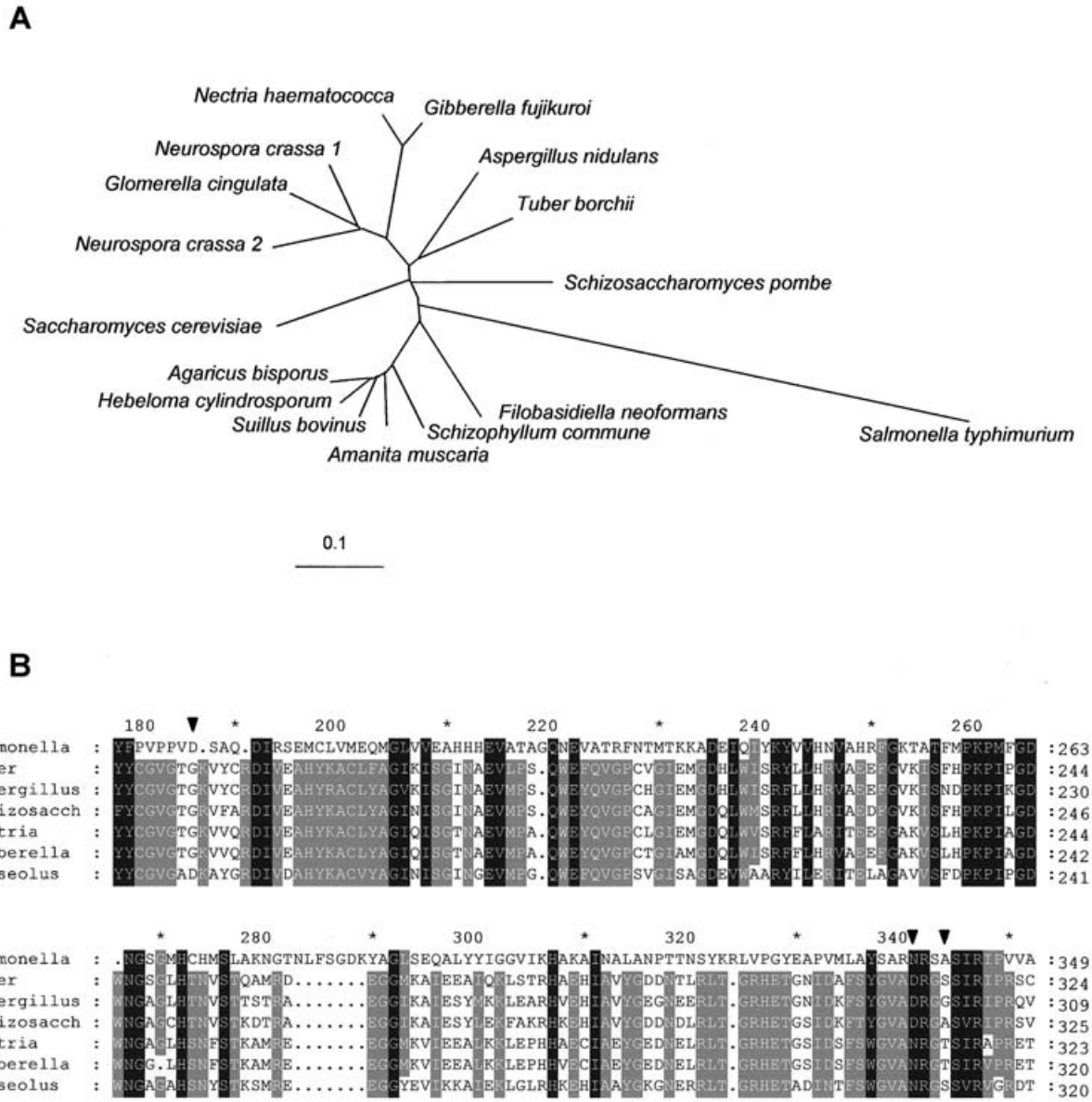

Figure 1 Relationships among fungal GSs

(**A**) A radial phylogenetic tree was constructed by neighbour joining on the basis of the alignment of the TbGS amino acid sequence with all the available homologous sequences from other fungi. The sequence of the *Salmonella typhimurium* enzyme has been included for comparison; branches are drawn to scale (the scale bar corresponds to 0.1 changes per site). The accession numbers of the sequences utilized for tree construction are: AF462037 (*T. borchii*); O00088 (*Agaricus bisporus*); CAD22045 (*Amanita muscaria*); AAK70354 (*Aspergillus nidulans*); CAD10037 (*Filobasidiella neoformans*); CAC27836 (*Gibberella fujikuroi*); Q12613 (*Glomerella cingulata*); AAK96111 (*Hebeloma cylindrosporum*); AAD52617 (*Nectria haematococca*); NCU06724.1 (*Neurosprora crassa 1*); NCU04856.1 (*N. crassa 2*); P32288 (*Saccharomyces cerevisiae*); 1301273A (*Salmonella typhimurium*); NP_593400 (*Schizosaccharomyces pombe*); AAF27660 (*Schizophyllum commune*); CAD48934 (*Suillus bovinus*). (**B**) A portion of the TbGS polypeptide sequence (positions 160–324; second row, right-hand side numbering) was aligned with the homologous regions of the prototypic GS from *S. typhimurium* (first row; uppermost and right-hand side numbering), with the cytosolic GS from *Phaseolus vulgaris* (accession AJFBQA) and with those of four GS sequences from ascomycetous fungi (position numbers for each sequence portion are shown on the right-hand side; see above for accession numbers). Amino acid residues that are conserved in all six sequences or in at least five of them are shown on a black or grey background, respectively. Arrowheads point to amino acid residues that are either partially or completely conserved among fungal GSs, but diverge from those present at the corresponding positions of the *S. typhimurium* enzyme. Gaps introduced to optimize the alignment are indicated by dots; positions corresponding to a 10-amino-acid-residue spacing are indicated by asteriks.

RESULTS

Isolation and sequence analysis of the TbGS cDNA

A 237-bp-long cDNA fragment highly similar in sequence to GS from yeast was initially isolated by homologous PCR amplification of a *T. borchii* mycelium cDNA library. This cDNA was subsequently found to be alignable with a cDNA insert picked randomly from the same library in the course of a *T. borchii* mycelium EST screening [10]. The latter cDNA, here designated TbGS (accession no. AF462037), was entirely sequenced and found to contain a 1077-nt-long open reading frame starting with an initiator ATG preceded by two in-frame stop codons and lying in a good sequence context according to translation-initiation rules in fungi. The translation product of this open reading frame was 358 amino acids long, with a predicted molecular mass of 39.7 kDa, which is in the same range as those reported

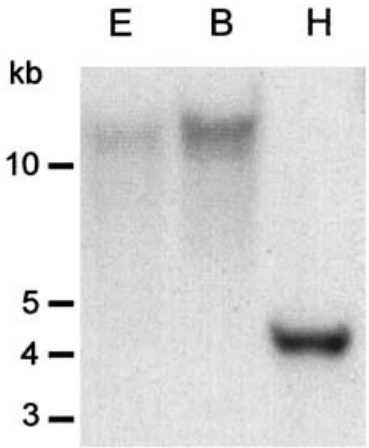

Figure 2 DNA gel-blot analysis of TbGS

T. borchii genomic DNA digested with *Eco*RI (E), *Bam*HI (B) or *Hin*dIII (H) was probed with a ^{32}P-labelled TbGS cDNA fragment derived from pGEM-*TbGS_237*. The migration positions of DNA size markers run alongside are indicated on the left.

previously for other eukaryotic GSs (34–43 kDa) [4,5,23–25]. As apparent in Figure 1(A), two main basidiomycete and ascomycete groups are discernible within the fungal GS cluster. TbGS belongs to an ascomycete subgroup made up entirely of filamentous ascomycetes, with a sequence from *Aspergillus nidulans* [26] as its closest homologue.

Comparative sequence analysis of the TbGS polypeptide towards homologous sequences from other prokaryotic and eukaryotic organisms reveals a substantial degree of sequence conservation throughout the entire sequence, consistent with the fact that this protein is considered a good molecular clock in evolution [27]. All 16 active-site residues and 31 of the 34 amino acid residues lying outside of the active-site region that have been proposed to be conserved in all species [5] are also conserved in TbGS. The three residues within the latter group that are not conserved in TbGS, corresponding to residues Asp^{186}, Asn^{338} and Ala^{341} in the prototypic GS sequence from *Salmonella typhimurium*, are replaced by Gly^{167}, Asp^{313} and Ser^{316}, respectively, in TbGS (Figure 1B). Some of these changes (like Gly^{167}) are conserved in all available fungal GS sequences. Other changes are instead shared only with a subset of fungal GS sequences (e.g. Asp^{313} in TbGS is present at the same position in the *A. nidulans* and in the *S. pombe* polypeptides [28], whereas Ser^{316} is conserved in the *S. pombe* sequence, but it is replaced by a glycine residue in *A. nidulans* or by a threonine residue in *Nectria haematococca* and *Gibberella fujikuroi*). Most of the remaining residues that have been proposed to be conserved in all eukaryotes [5] are also conserved in TbGS (107 out of 134 amino acid residues).

RNA and DNA gel-blot analysis

An mRNA of ≈1300 nt was identified by an RNA gel-blot analysis conducted with the cDNA fragment (237 bp) initially isolated by PCR amplification (results not shown). The same cDNA probe was utilized for DNA gel-blot analysis, which was conducted on *T. borchii* genomic DNA digested with restriction enzymes (*Eco*RI, *Bam*HI and *Hin*dIII) that do not cut within the TbGS cDNA. As shown in Figure 2, a single-band hybridization pattern was obtained with genomic DNA digested with either enzyme and hybridized with the TbGS cDNA probe under low-

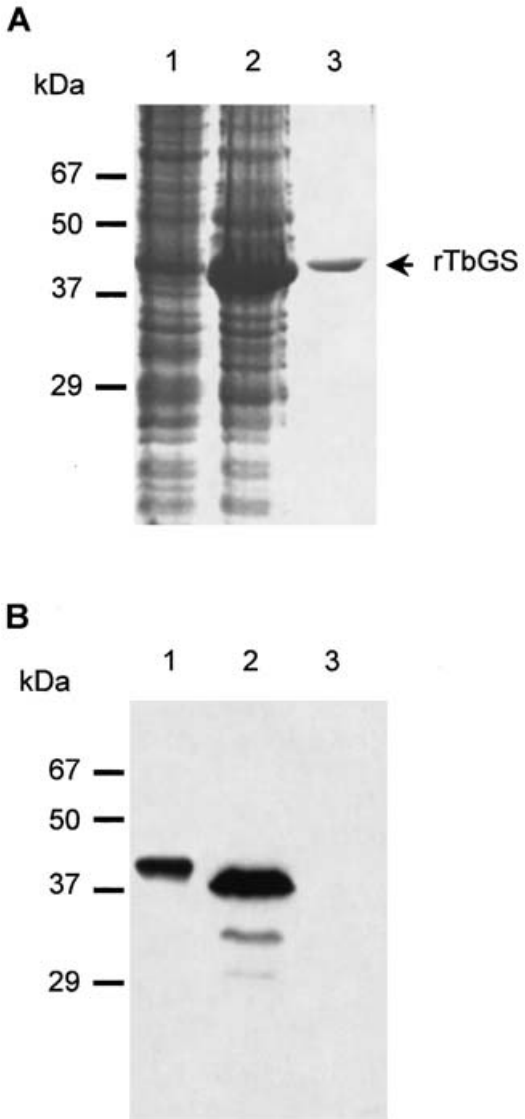

Figure 3 Bacterial expression, purification and immunoblot analysis of TbGS

(**A**) SDS/PAGE of total lysates from uninduced (lane 1) or isopropyl β-D-thiogalactoside-induced (lane 2) bacterial cells carrying the pET-*TbGS* plasmid, and of metal-affinity-purified (His-tagged) rTbGS (lane 3). (**B**) Immunodetection of recombinant (lane 1) and natural (lane 2) TbGS; a control reaction carried out with the pre-immune serum is shown in lane 3. The migration positions of molecular-mass markers and of rTbGS are indicated.

stringency conditions. GS thus appears to be encoded by a single-copy gene in the *Tuber* genome.

Functional characterization of the recombinant TbGS protein

To verify the ability of the *TbGS*-encoded protein to support glutamine synthesis, the *T. borchii* polypeptide was expressed in *E. coli* as an N-terminal fusion with a metal-binding hexahistidine tag. The resulting recombinant protein (rTbGS), which was obtained in high amounts in a soluble form and was identified initially with the use of a monoclonal anti-His tag antibody (results not shown), was purified to near homogeneity as a single polypeptide of ≈42 kDa (Figure 3A). This protein preparation was utilized for activity assays and for the production of polyclonal anti-TbGS antibodies. As shown in Figure 3(B),

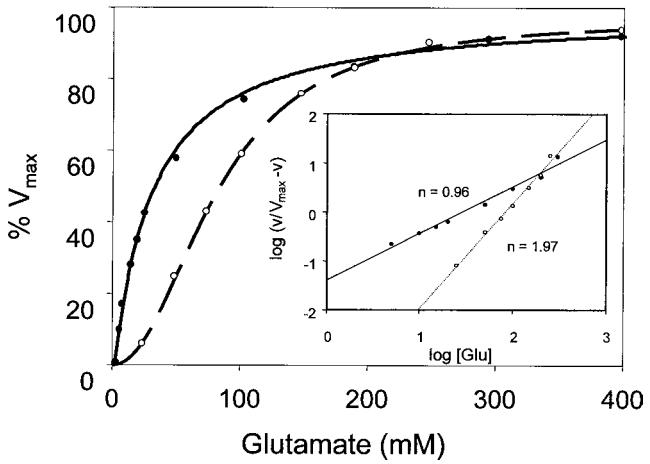

Figure 4 Enzyme kinetics for L-glutamate

Biosynthetic GS activity assays were carried out as described in the Materials and methods section, varying the concentration of L-Glu in the reaction mixture. Plots of *v* versus [S] are shown for rTbGS (○). For comparative purposes the results of a similar experiment with recombinant (6 × His-tagged) plant GS from *Phaseolus vulgaris* are also shown (●). Velocity data, expressed as percentages of V_{max}, are the mean of two sets of determinations that differed by no more than 10 % of the mean; absolute V_{max} values were 14.15 and 8.05 nmol of $P_i \cdot min^{-1} \cdot \mu g$ of GS^{-1} for the *Tuber* and the plant enzymes, respectively. Inset: Hill plots of the data obtained with TbGS (○; $h = 1.97$, $r^2 = 0.996$) and with *Phaseolus* GS (●; $h = 0.96$, $r^2 = 0.991$).

three polypeptides were recognized specifically by the anti-TbGS antiserum in a crude cytosolic extract from *Tuber* mycelia. This size heterogeneity, which was attenuated partially (but not abolished completely) by the inclusion of protease inhibitors in the extraction buffer, is probably due to artificial proteolytic degradation of the enzyme during extract preparation. In fact, the size of the largest and most abundant of such polypeptides (≈40 kDa) is very close to that predicted by sequence analysis, and it is also about the same as that of the single immunoreactive polypeptide revealed by immunoblot analysis of purified rTbGS, which carries a 20-amino-acid extension at the N-terminus. At variance with its single-band SDS/PAGE pattern, recombinant TbGS was resolved into two main peaks upon non-denaturing gel-filtration analysis (results not shown); one peak, corresponding to about 40 % of the total protein applied to the column, eluted with an apparent molecular mass of 340 kDa, whereas the other eluted with an apparent molecular mass of 175 kDa. A similar result, with a slightly larger proportion of the high-molecular-mass species, was also obtained by non-denaturing gel-electrophoretic analysis of rTbGS (results not shown). In accordance with native size estimates reported previously for GSs from other eukaryotic sources [5], it thus appears that under non-denaturing conditions TbGS is present as a mixture of homo-oligomers composed by either four or eight identical subunits.

In preliminary experiments carried out under standard biosynthetic reaction assay conditions (see the Materials and methods section), purified rTbGS was found to be catalytically active and to respond linearly both to protein amount (up to 500 ng) and incubation time (up to 60 min at 37 °C) with specific activity values (5–7 units/mg) in the same range as those reported previously for other recombinant GSs probed with the same type of assay [19,29,30]. These initial measurements were followed by the specific optimization of GS activity and by a systematic analysis of the dependence of *Tuber* GS on the concentrations of ammonium, glutamate, ATP and Mg^{2+}, all tested at an optimum pH of 7.5. A strong positive co-operativity ($h = 1.7 \pm 0.29$) and a fairly high $S_{0.5}$ value (54 ± 16 mM; $S_{0.5}$ is the substrate concentration value at which $v = \frac{1}{2}V_{max}$) were measured in the case of the glutamate co-substrate (Figure 4). Instead, no co-operativity, or only a slight (but reproducible) positive co-operativity, was observed in the case of NH_4^+ and ATP, or Mg^{2+}, respectively (results not shown). Also, no product inhibition was observed following glutamine supplementation up to a concentration of 75 mM. The resulting kinetic parameters, along with the half-inhibitory concentrations of the two glutamate analogues L-methionine sulphoximine (MSX; 47 mM) and L-phosphinothricin (PPT; 0.5 mM), are reported in Table 1. As expected on the basis of the relatively low affinity of glutamate, both compounds were found to have IC_{50} values considerably higher than those reported previously for other fungal and plant GSs [4,5,31]. In fact, a non-allosteric response to increasing concentrations of glutamate was observed under the same reaction conditions for a recombinant (His-tagged), cytosolic homopolymeric α-GS from *Phaseolus vulgaris*, with a K_m for glutamate of 15 mM and IC_{50} values of 0.5 and 0.0025 mM for MSX and PPT, respectively (Figure 4 and results not shown).

Table 1 Kinetic parameters of TbGS

GS activity was measured with the biosynthetic reaction assay as specified in the Materials and methods section. Under optimized reaction conditions (10 s at 37 °C, pH 7.5, with 250 ng of rTbGS), the V_{max} of homogeneously purified rTbGS was 14.2 ± 2.3 nmol of $Pi \cdot min^{-1} \cdot \mu g$ of $protein^{-1}$; the results are means ± S.D. from at least three independent experiments. ND, no inhibition by L-glutamine (L-Gln) was detected up to a concentration of 75 mM.

Kinetic parameter	Value (mM)
K_m for ATP	0.17 ± 0.043
K_m for NH_4^+	0.75 ± 0.12
$S_{0.5}$ for L-Glu	54 ± 15.9 ($n = 1.7 \pm 0.29$)
$S_{0.5}$ for Mg^{2+}	6.7 ± 2.50 ($n = 1.17 \pm 0.042$)
IC_{50} for MSX	47 ± 13.3
IC_{50} for PPT	0.5 ± 0.09
IC_{50} for L-Gln	ND

TbGS modulation in mycelia cultured under different N-nutritional regimens

RNA gel-blot and RNase-protection assays were conducted to determine the steady-state levels of the TbGS mRNA in *T. borchii* mycelia subjected to different nutritional perturbations. The RNA gel-blot data reported in Figure 5(A) show that the TbGS messenger slowly increased following transfer of N-sufficient mycelia to an N-deprived SSM and rapidly returned to basal levels upon N resupplementation. The extent of such up-regulation, which was maximal after 21 days of starvation, was 6-fold with respect to unshifted 21-day-old mycelia (t_0 control), but about 2-fold less if compared with TbGS mRNA levels in parallel, mock-shifted mycelia cultured for an additional 21 days in N-sufficient SSM prior to RNA extraction. TbGS mRNA levels in such MSCs were about the same as those measured in parallel mycelial cultures deprived of either glucose or phosphate (results not shown). Similar results, as to the extent and the time course of TbGS modulation following deprivation and subsequent resupplementation of ammonium, were obtained with mycelia that had been pre-cultured in SSM for 10 (rather than 21) days prior to N downshift (results not shown). As shown further in Figures 5(B) and 5(C), TbGS mRNA derepression following N deprivation and the reverse response induced by N resupplementation were closely paralleled by both GS protein and enzyme-activity levels, thus indicating that the observed N-status-dependent responses derive mainly from transcriptional

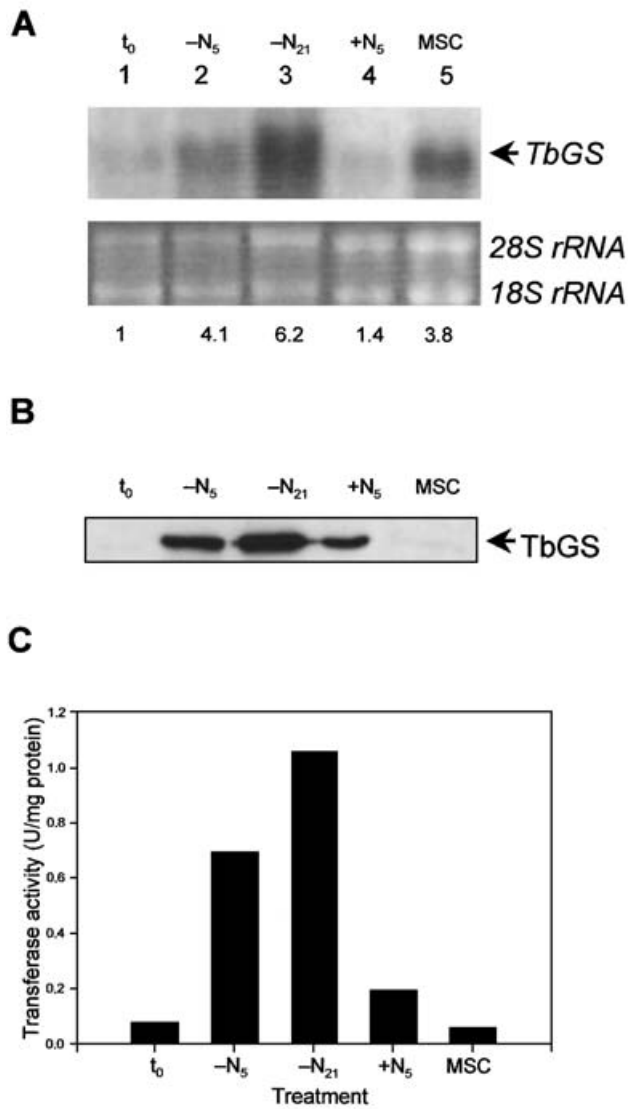

Figure 5 N-status-dependent modulation of TbGS

(**A**) Gel-blot analysis of the TbGS mRNA in mycelia grown for 21 days on complete SSM (t_0; lane 1) and then transferred for 5 ($-N_5$; lane 2) or 21 ($-N_{21}$; lane 3) days to a modified SSM lacking any source of nitrogen. TbGS mRNA levels in parallel mycelial cultures, N-starved for 21 days and then transferred for 5 days to N-sufficient SSM are shown in lane 4 ($+N_5$); a parallel RNA gel-blot analysis conducted on mycelia grown for 21 days on SSM and then shifted for an equal length of time to the same medium (MSC) is shown in lane 5. Ethidium bromide-stained rRNAs for each total RNA sample utilized for gel-blot analysis are shown at the bottom; they were quantified by densitometric analysis and used as internal standards. Relative TbGS levels, normalized with respect to unshifted t_0 controls (lane 1), were determined for each of the above conditions and are reported below the corresponding lanes. (**B**) Immunoblot analysis of TbGS protein levels in soluble extracts derived from mycelia cultured under each of the above-listed conditions. (**C**) GS activity levels (measured with the transferase reaction assay, see the Materials and methods section for details) in the same mycelial extracts utilized for the experiments reported in (**B**). Data are from a representative experiment that was performed twice and analysed in duplicate with results differing by no more than 15 % of the mean.

up-regulation or reduced turnover of the TbGS messenger. The sole exception to this internally consistent pattern of mRNA and protein/enzyme-activity levels was found in the case of mock-shifted mycelia, which despite significant mRNA up-regulation (compare lanes 1 and 5 in Figure 5A) had enzyme-activity and GS protein levels comparable with those of t_0 controls (compare t_0 and MSC in Figures 5B and 5C).

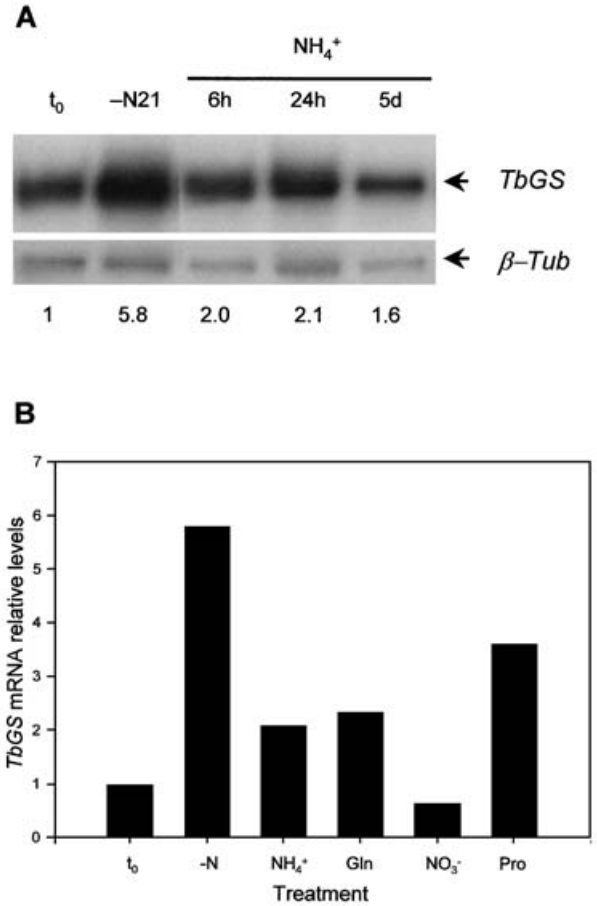

Figure 6 TbGS down-regulation following nitrogen resupplementation of N-starved mycelia

(**A**) RNase-protection analysis of the TbGS mRNA in mycelia pre-cultured for 21 days on complete SSM (t_0), transferred for an additional 21-day period to N-deprived SSM ($-N_{21}$), and further shifted for the times indicated above each lane to a modified SSM containing 4 mM NH_4Cl as the sole source of nitrogen. A *T. borchii* β-tubulin (β-Tub) antisense riboprobe was included in all assays as an internal standard. The bands shown, which correspond to full-length protection products of the TbGS and β-tubulin riboprobes, were visualized by autoradiography and quantified by phosphorimaging. Relative TbGS levels (reported below each lane) were calculated by dividing the volumes of the TbGS signals by the volumes of the corresponding β-tubulin signals, followed by normalization with respect to the same type of ratio measured in t_0 controls. (**B**) Relative TbGS levels in mycelia cultured for 21 days in the absence of any N source under the above-described conditions ($-$N), and then transferred for 24 h to modified SSMs containing NH_4Cl (NH_4^+), KNO_3 (NO_3^-), L-glutamine (Gln) or L-proline (Pro; each at 4 mM final concentration) as sole N sources. Data analysis and quantification were performed as in (**A**); relative TbGS levels, normalized with respect to the t_0 control, are reported on the *y* axis.

The reverse response, i.e. TbGS down-regulation following resupplementation of various N sources, was then investigated in more detail by RNase-protection assays. The results of the time-course experiment reported in Figure 6(A) show that TbGS down-regulation following ammonium refeeding was rather fast and substantial, and nearly basal TbGS mRNA levels were recovered within 6 h from ammonium resupplementation. As revealed by the results of a similar experiment comparing different N sources at a fixed post-resupplementation time (Figure 6B), L-proline barely affected TbGS expression levels and glutamine had nearly the same down-regulation capacity as ammonium, whereas nitrate behaved as the most effective nitrogen source, leading rapidly to TbGS mRNA levels that were actually lower than those measured in nitrogen (NH_4^+)-sufficient t_0 controls.

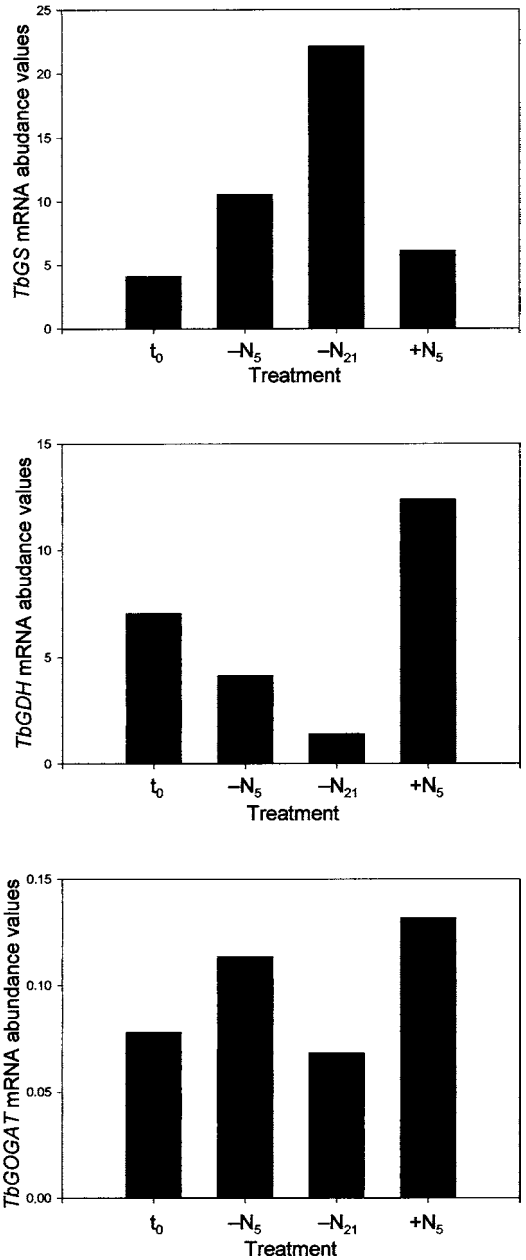

Figure 7 Relative abundance of TbGS, TbGDH and TbGOGAT in mycelia subjected to different N-nutritional regimens

The data summarize the results of a comparative RNase-protection analysis of TbGS, TbGDH and TbGOGAT mRNAs, conducted on N-sufficient 21-day-old mycelia (t_0), on parallel mycelia further cultured for 5 ($-N_5$) or 21 ($-N_{21}$) days under N-deprivation conditions, and on a subset of mycelia returned to N-sufficient SSM for 5 days ($+N_5$; see the Materials and methods section for details on the specific activity of the ^{32}P-labelled riboprobes utilized for this experiment). Values reported on the *y* axes are relative transcript abundance values, not normalized with respect to the t_0 condition, that were calculated by dividing the volumes of the TbGS, TbGDH and TbGOGAT signals by the volumes of the corresponding β-tubulin signals.

mRNA expression profiling of TbGS and other N-assimilation enzymes in mycelia and fruitbodies

Considering the ability of GS to drive N assimilation in concert with either GDH or GOGAT (or both), we next compared the above-described TbGS mRNA responses with those of the mRNAs coding for the latter two enzymes. As revealed by the results of the RNase-protection assays reported in Figure 7,

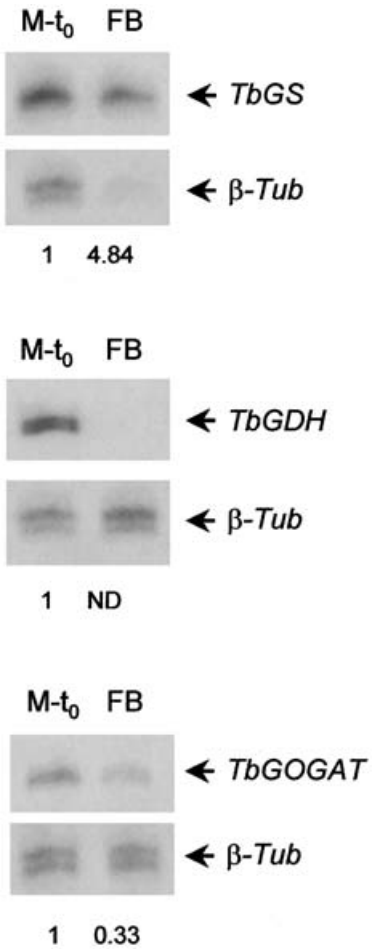

Figure 8 TbGS, TbGDH and TbGOGAT expression levels in *Tuber* fruitbodies

RNase-protection assays were conducted in parallel on 21-day-old, N-sufficient mycelia (M-t_0) and on 80% mature fruitbodies (FB). Data analysis and quantification were performed as specified in the legend to Figure 6. Relative expression levels, normalized with respect to t_0 mycelia (M-t_0), are reported below each lane. The same exposure time was used for autoradiography of the TbGS, TbGDH and β-tubulin transcripts; a longer exposure time was employed for TbGOGAT visualization.

the expression profiles displayed by these two mRNAs differ substantially from those of the TbGS messenger. A qualitatively opposite response, with a marked repression under N-starvation conditions and a prompt up-regulation following ammonium refeeding, was observed in the case of the TbGDH mRNA. The TbGOGAT messenger, instead, was expressed at similar levels (with no more than a 2-fold variation) under different N status conditions. Also apparent in Figure 7 are the different relative abundance values of the three messengers (i.e. the ratio between the hybridization signal for a certain N-assimilation component mRNA and the signal for the β-tubulin internal standard mRNA under a given condition). The TbGS mRNA was 16-fold more abundant than the TbGDH mRNA in N-starved mycelia, the TbGDH mRNA was $\approx$2-fold more abundant than the TbGS mRNA under N-sufficient conditions (both at t_0 and after ammonium refeeding), whereas the constitutively expressed TbGOGAT messenger was the least represented under either condition.

RNase-protection assays were also used to determine the levels of the TbGS, TbGDH and TbGOGAT messengers in *Tuber* fruitbodies. As shown in Figure 8, the TbGS mRNA was

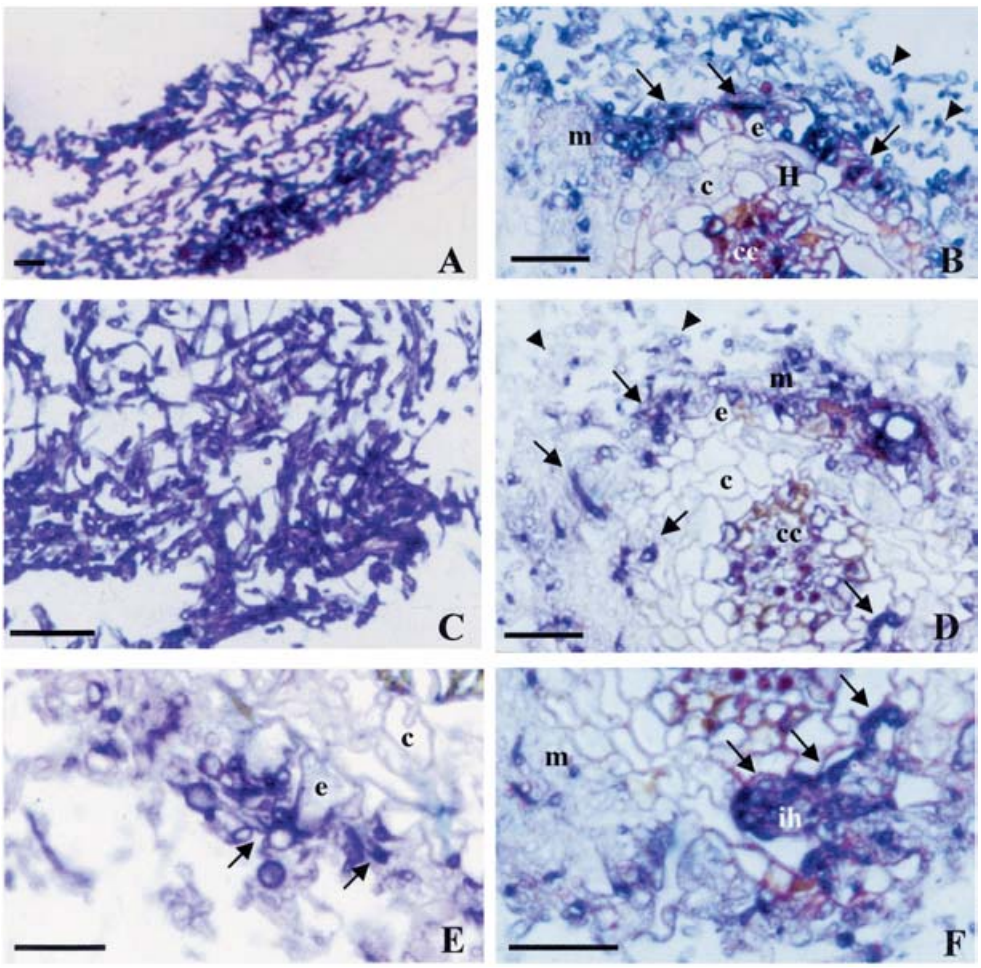

Figure 9 ***In situ*** **hybridization analysis of the TbGS mRNA**

(**A**) Hyphae from a free-living, 30-day-old mycelium hybridized with the antisense, digoxygenin-labelled 18 S rRNA probe. (**B**) Hybridization of the antisense 18 S rRNA probe with a fully differentiated *Tuber*/linden mycorrhiza. The strong hybridization signals observed in mantle-forming hyphae (arrows) contacting the root surface, and in a few extramatrical hyphae (arrowheads) are indicated. (**C**) Hyphae from the same mycelium shown in (**A**) hybridized with the digoxygenin-labelled antisense TbGS probe. (**D**) Hybridization of a transversal section of the same ectomycorrhiza utilized for the experiment in (**B**) with the antisense TbGS riboprobe. A strong signal is observed in several hyphae of the mycorrhizal network, especially in the inner part of the mantle (arrows); extramatrical hyphae (arrowheads) are only slightly reactive. (**E**) Detail of an ectomycorrhiza sampled in a very early stage of the interaction; arrows point to an intense signal in the cytoplasm of extramatrical hyphae contacting the root surface. (**F**) In a fully differentiated mycorrhiza, a strong TbGS mRNA hybridization signal is evident in large, coiled hyphae penetrating among and within root cells (arrows). Scale bars correspond to 40 μm (**A**–**D**, **F**) and 20 μm (**E**). e, root epidermal cell; c, root cortical cell; cc, central cylinder; H, Hartig net; ih, intracellular hyphae; m, mantle.

significantly (≈5-fold) more represented in fruitbodies than in N-sufficient mycelia and the TbGOGAT messenger was about 3-fold more abundant in mycelia than in fruitbodies, whereas the TbGDH mRNA was undetectable in fruitbodies even at longer autoradiographic exposures.

In situ hybridization analysis of the TbGS mRNA in mycorrhizae

Because of the simultaneous presence of plant and fungal cells in the symbiotic tissue, a different experimental approach, RNA *in situ* hybridization, was used to analyse the expression and tissue distribution of the TbGS mRNA in *Tuber*/linden (*Tilia platyphyllos*) mycorrhizae. To obtain a comparative estimate of TbGS abundance and distribution, parallel *in situ* hybridization experiments, using digoxygenin-labelled 18 S rRNA or TbGS mRNA antisense riboprobes, were conducted on sections prepared from free-living mycelia grown for 30 days in a synthetic liquid medium (Figures 9A and 9C) or from ectomycorrhizae (Figures 9B and 9D–9F). The 18 S rRNA riboprobe, that was used as a positive control for these experiments, produced a strong hybridization signal in the cytoplasm of both free-living (Figure 9A) and symbiosis-engaged (Figure 9B) hyphae, including extramatrical hyphae as well as root-ensheathing (mantle) hyphae and hyphae forming the nutrient-exchange interface (Hartig net) between the fungus and the plant. A fairly strong cytoplasmic signal was detected similarly in sections of either free-living or symbiotic hyphae after treatment with the 'antisense' TbGS riboprobe (Figures 9C and 9D). As revealed by the hybridization patterns obtained with ectomycorrhizae, the TbGS probe was absolutely fungus-specific and no labelling of plant tissues was ever observed. Similarly, no signal was detected in control experiments carried out with a 'sense' TbGS riboprobe, regardless of the saprotrophic or symbiotic state of the fungus (results not shown).

Different stages of plant–fungus interaction were then investigated. In young mycorrhizal roots, where hyphae proliferate at the root surface, contact epidermal cells, and later

grow among these cells, the TbGS hybridization signal was most evident in extramatrical hyphae growing around the root as well as in hyphae contacting epidermal root cells (Figure 9E). A similar pattern, with a diffuse hybridization signal in the cytoplasm of mantle and Hartig net-forming hyphae, was detected in fully differentiated ectomycorrhizae (Figure 9F). In this case, however, a strong additional signal was reproducibly observed in large, coiled hyphae penetrating within root cells (marked with arrows in Figure 9F).

DISCUSSION

Properties of TbGS

A single gene in the *Tuber* genome codes for a GS polypeptide that autonomously assembles into catalytically active homo-oligomers. This contrasts, for example, with the situation in the related filamentous ascomycete *Neurospora crassa*, where two different GS subunits were first identified by PAGE analysis [32], and subsequently shown to be encoded by two distinct genes [33]. Various features of the *Tuber* enzyme agree fairly well with those of natural or recombinant GSs from other eukaryotic organisms [19,20,34,35]. The most peculiar kinetic parameters were the fairly high $S_{0.5}$ for glutamate, the unusually high IC_{50} values for the glutamate analogues MSX and PPT, and the positive co-operativity towards this substrate, even though comparable K_m values for L-glutamate (in the 23–46 mM range) have been measured previously for GSs from other sources [36–38]. These functional peculiarities of the *Tuber* enzyme are probably related to some of the specific amino acid replacements found in the TbGS polypeptide (Figure 1B). For example, a highly conserved residue corresponding to Asn^{338} in the prototypical enzyme from *S. typhimurium* is replaced by Asp^{313} in TbGS. This asparagine is next to Arg^{339}, an active-site residue that is close to a polypeptide region involved in the interaction with glutamate and its analogues. In addition, Arg^{339} was shown to be involved in intersubunit contact stabilization [5]. Therefore it is likely that amino acid replacements around this region of TbGS are related to the tendency of the *Tuber* enzyme to display a tetrameric quaternary structure *in vitro*, in addition to the more characteristic octameric structure of eukaryotic GSs. Indeed, the occurrence of catalytically active tetrameric forms is quite common among GSs from various eukaryotes, including *Saccharomyces cerevisiae* [39] and *N. crassa*, where changes in quaternary structure (i.e. the replacement of a 'basal' octameric GS with a highly active tetrameric form under N-limiting conditions) have been shown to be involved in GS activity regulation in response to perturbations of the N status [40].

The apparent K_m for ammonium of TbGS is 3–5-fold lower than the intracellular NH_4^+ concentration found in other ectomycorrhizal fungi, whereas the corresponding value for glutamate exceeds by about 5-fold the highest intracellular glutamate concentration found previously in the ectomycorrhizal basidiomycete *Laccaria laccata* [4]. If such a gap between the apparent $S_{0.5}$ and the intracellular concentration of glutamate holds for the *Tuber* enzyme under conditions *in vivo*, it may indicate that TbGS is set to work at rates that are well below its maximum biosynthetic capacity. This would allow other fungal enzymes involved in amino acid metabolism (e.g. glutamate/pyruvate transaminase, whose mRNA exhibits the same type of N-starvation response as TbGDH; B. Montanini and S. Ottonello, unpublished work) as well as glutamate-utilizing plant enzymes to compete for this amino acid under conditions of N sufficiency, while relying on biosynthetic TbGS up-regulation to respond to conditions of persistent N limitation. It is also possible, however, that additional mechanisms positively regulate TbGS activity under conditions *in vivo*. For example, a phosphorylation-driven interaction with 14-3-3 proteins leading to enzyme activation and stabilization against proteolytic cleavage has been reported recently for plant GSs [41,42]. Notably, a putative 14-3-3 interaction motif, Arg-Ser-Lys-Thr-Lys-Thr, in which the fourth residue (underlined) represents the phosphorylation site, is present in TbGS between positions 40 and 45.

N status-dependent modulation of TbGS

The TbGS mRNA responded positively to N deprivation and returned rapidly to basal levels upon resupplementation of various forms of nitrogen (especially nitrate). Both responses were accompanied by parallel variations of TbGS protein and enzyme-activity levels, thus indicating that TbGS derepression under N-limiting conditions, and the reverse response following N resupplementation, take place mainly at the pre-translational level. The sole exception to this concerted mRNA/protein response was found in mock-shifted 42-day-old mycelia (Figure 5), where the TbGS messenger accumulated in a non-translatable form leading to barely detectable protein and enzyme-activity levels (similar to those of unshifted t_0 controls). Compared with GS modulation in other fungi [8,9], the two most peculiar features of *Tuber* GS are its extremely slow biosynthetic derepression and the lack of product inhibition by glutamine. As suggested by the identical time course of response we have documented recently for the high-affinity NH_4^+ transporter *T. borchii* AMT1 [12] and for the NO_3^- transporter (B. Montanini and S. Ottonello, unpublished work), this delayed (yet strictly co-ordinate) up-regulation seems to be a specific feature of the N-assimilation components from *Tuber*. In fact, much faster N-deprivation responses are displayed by functionally homologous components (including GS) in other ectomycorrhizal fungi [43,44] as well as by *Tuber* surface components not directly related to N metabolism, such as the TbSP1 phospholipase [16]. This suggests that indirect surface remodelling events (rather than true metabolic adaptation) are dominating the response to N starvation in *Tuber* mycelia.

GS is the primary ammonium-assimilating component in N-starved mycelia and in fruitbodies

An opposite response to N starvation, compared with that of the TbGS mRNA, was observed for the TbGDH mRNA, whereas the TbGOGAT messenger was found to be expressed in a seemingly constitutive manner in both N-deprived and N-sufficient mycelia. Consistent with our mRNA-expression data, a high prevalence of GS over GDH and a quantitatively important contribution of the GS/GOGAT cycle to N assimilation have been documented previously in other filamentous fungi [4]. It thus appears that in *Tuber* mycelia GS, rather than GDH, is the primary NH_4^+-assimilating enzyme under N-limiting conditions (probably resembling those experienced by free-living mycelia in the soil) and that the GS/GOGAT cycle (the main glutamate biosynthetic pathway in plants) is the preferred route of NH_4^+ assimilation in this organism.

In keeping with this view, a qualitatively similar, but even more discriminating expression pattern – with practically undetectable levels of TbGDH – was observed in fruitbodies, a life-cycle stage that is thought to be metabolically active, yet naturally subjected to a fairly strong nutrient limitation [11]. Also, GS has been found recently to be the most highly expressed among 41 mRNAs displaying a substantial up-regulation during

the mycelium/fruitbody transition in *Tuber* [10]. This marked TbGS accumulation points to additional roles, besides basal N assimilation as in free-living mycelia, that GS may play in more specialized life-cycle stages such as fruitbodies. Indeed, an increase in GS activity was observed previously in developing basidiomata of *Coprinus cinereus*, where it was causally related to the accumulation of osmotically active compounds such as urea and arginine that may contribute to cellular expansion, as well as to a more effective utilization (and concomitant depletion) of NH_4^+, a powerful inhibitor of meiosis [11,45].

TbGS expression in mycorrhizae

Overall TbGS hybridization signals in mycorrhizae were found to be comparable with those of free-living mycelia cultured for 30 days in a synthetic liquid medium under progressively more limiting N-availability conditions. This suggests that TbGS mRNA levels in symbiotic hyphae may be closer to those of partially derepressed, N-limited mycelia than to the basal levels found in N-sufficient mycelia. Whether the GS/GOGAT or the GDH/GS pathway is primarily responsible for glutamine/glutamate biosynthesis within *Tuber* mycorrhizae is presently unknown. It is interesting to note, however, that at variance with the situation in fruitbodies, low levels of the TbGDH mRNA (compared with mycelia) have been detected recently in *Tuber* mycorrhizae [15].

Given the extremely low sensitivity of TbGS to the widely used herbicide phosphinothricin (also known as glufosinate) and its relatively high expression levels in symbiotic hyphae, it is conceivable to imagine that *Tuber* mycorrhizae may afford protection against otherwise lethal concentrations of this compound to their host plants. The other new information provided by *in situ* hybridization analysis is that in fully differentiated *Tuber* mycorrhizae the TbGS signal is most intense within large hyphae that are penetrating within root cells. The presence of intracellular hyphae in an ectomycorrhiza is not completely unexpected, since *T. borchii*, like other mycorrhizal ascomycetes, can easily colonize the epidermal root cells of its hosts (P. Bonfante and R. Balestrini, unpublished work). What is perhaps more surprising is that TbGS mRNA signals were much more intense in such hyphae than in other mycorrhizal compartments. Considering the fairly strong TbGS down-regulating capacity of glutamine (Figure 6B) and its role as the major form of N transferred from the fungus to the plant [4], one might imagine that this cell-specific TbGS up-regulation is due to an increased glutamine depletion in cortex-penetrating hyphae, resulting from a more efficient mobilization of this amino acid towards the phytobiotic sink. In fact, similar to the situation in rhizobial bacteroids, which release ammonium to the plant through the surrounding peribacteroid membrane [46], the internalization of the fungus might help to create a more favourable nutrient-exchange interface between the two symbiotic partners.

We thank Angelo Viotti and Barbara Lazzari (Istituto di Biologia e Biotecnologia Agraria, CNR, Milan, Italy) for the *Tuber* cDNA library, and Davide Sisti (Istituto Botanico, University of Urbino, Urbino, Italy) for the gift of ectomycorrhiza samples. The help of Elisabetta Soragni and Marco Busconi (Department of Biochemistry and Molecular Biology, University of Parma) in an early phase of this work is also gratefully acknowledged. This work was supported by grants from the National Research Council of Italy (Progetto Strategico "Biotecnologia dei funghi eduli ectomicorrizici"), from the Ministry of Education, University and Research (FIRB), and by a grant from the Regione Emilia-Romagna. M. B. and A. J. M. acknowledge additional support from the European Union (HPRN-CT2000-00086).

REFERENCES

1 Martin, F., Cliquet, J. B. and Stewart, G. (2001) Nitrogen acquisition and assimilation in mycorrhizal symbioses. In The Assimilation of Nitrogen in Plants (Lea, P. and Morot-Gaudry, J. F., eds.), pp. 147–166, Springer-Verlag, Berlin
2 Read, D. J. (1999) Mycorrhiza – the state of the art. In Mycorrhiza: Structure, Function, Molecular Biology and Biotechnology (Varma, A. and Hock, B., eds.), pp. 3–34, Springer-Verlag, Berlin
3 Buscot, F., Munch, J. C., Charcosset, J. Y., Gardes, M., Nehls, U. and Hampp, R. (2000) Recent advances in exploring physiology and biodiversity of ectomycorrhizas highlight the functioning of these symbioses in ecosystems. FEMS Microbiol. Rev. **24**, 601–614
4 Botton, B. and Chalot, M. (1999) Nitrogen assimilation: enzymology in ectomycorrhizas. In Mycorrhiza: Structure, Function, Molecular Biology and Biotechnology (Varma, A. and Hock, B., eds.), pp. 333–372, Springer-Verlag, Berlin
5 Eisenberg, D., Gill, H. S., Pfluegl, G. M. and Rotstein, S. H. (2000) Structure-function relationships of glutamine synthetases. Biochim. Biophys. Acta **1477**, 122–145
6 Oaks, A. and Hirel, B. (1985) Nitrogen metabolism in roots. Annu. Rev. Plant Physiol. **36**, 345–365
7 Marzluf, G. A. (1997) Genetic regulation of nitrogen metabolism in the fungi. Microbiol. Mol. Biol. Rev. **61**, 17–32
8 Sims, A. P., Toone, J. and Box, V. (1974) The regulation of glutamine synthesis in the food yeast *Candida utilis*: the purification and subunit structure of glutamine synthetase and aspects of enzyme deactivation. J. Gen. Microbiol. **80**, 485–499
9 Legrain, C., Vissers, S., Dubois, E., Legrain, M. and Wiame, J. M. (1982) Regulation of glutamine synthetase from *Saccharomyces cerevisiae* by repression, inactivation and proteolysis. Eur. J. Biochem. **123**, 611–616
10 Lacourt, I., Duplessis, S., Abba, S., Bonfante, P. and Martin, F. (2002) Isolation and characterization of differentially expressed genes in the mycelium and fruit body of *Tuber borchii*. Appl. Environ. Microbiol. **68**, 4574–4582
11 Moore, D. (1998) Fungal morphogenesis, Cambridge University Press, Cambridge
12 Montanini, B., Moretto, N., Soragni, E., Percudani, R. and Ottonello, S. (2002) A high-affinity ammonium transporter from the mycorrhizal ascomycete *Tuber borchii*. Fungal Genet. Biol. **36**, 22–34
13 Balestrini, R., Mainieri, D., Soragni, E., Garnero, L., Rollino, S., Viotti, A., Ottonello, S. and Bonfante, P. (2000) Differential expression of chitin synthase III and IV mRNAs in ascomata of *Tuber borchii* Vittad. Fungal Genet. Biol. **31**, 219–232
14 Giomaro, G., Zambonelli, A., Sisti, D., Cecchini, M., Evangelista, V. and Stocchi, V. (2000) Anatomical and morphological characterization of mycorrhizas of five strains of *Tuber borchii* Vittad. Mycorrhiza **10**, 107–114
15 Vallorani, L., Polidori, E., Sacconi, C., Agostini, D., Pierleoni, R., Piccoli, G., Zeppa, S. and Stocchi, V. (2002) Biochemical and molecular characterization of NADP glutamate dehydrogenase from the ectomycorrhizal fungus *Tuber borchii*. New Phytol. **154**, 779–790
16 Soragni, E., Bolchi, A., Balestrini, R., Gambaretto, C., Percudani, R., Bonfante, P. and Ottonello, S. (2001) A nutrient-regulated, dual localization phospholipase A2 in the symbiotic fungus *Tuber borchii*. EMBO J. **20**, 5079–5090
17 Laemmli, U. K. (1970) Cleavage of structural proteins during the assembly of the head of bacteriophage T4. Nature (London) **227**, 680–685
18 Pajuelo, E., Borrero, J. A. and Marquez, A. J. (1993) Immunological approach to subunit composition of ferredoxin-nitrite reductase from *Chlamydomonas reinhardtii*. Plant Sci. **95**, 9–21
19 Betti, M., Márquez, A. J., Yanes, C. and Maestre, A. (2002) ATP binding to purified homopolymeric plant glutamine synthetase studied by isothermal titration calorimetry. Thermochim. Acta **394**, 63–71
20 Clemente, M. T. and Marquez, A. J. (1999) Functional importance of Asp56 from the alpha-polypeptide of *Phaseolus vulgaris* glutamine synthetase. An essential residue for transferase but not for biosynthetic enzyme activity. Eur. J. Biochem. **264**, 453–460
21 Lanzetta, P. A., Alvarez, L. J., Reinach, P. S. and Candia, O. A. (1979) An improved assay for nanomole amounts of inorganic phosphate. Anal. Biochem. **100**, 95–97
22 Torres, M. A., Rigau, J., Puigdomenech, P. and Stiefel, V. (1995) Specific distribution of mRNA in maize growing pollen tubes observed by whole-mount *in situ* hybridization with non-radioactive probes. Plant J. **8**, 317–321
23 Brun, A., Chalot, M., Botton, B. and Martin, F. (1992) Purification and characterization of glutamine synthetase and NADP-glutamate dehydrogenase from the ectomycorrizal fungus *Laccaria laccata*. Plant Physiol. **99**, 938–944
24 Kersten, M. A., Muller, Y., Op den Camp, H. J., Vogels, G. D., Van Griensven, L. J., Visser, J. and Schaap, P. J. (1997) Molecular characterization of the glnA gene encoding glutamine synthetase from the edible mushroom *Agaricus bisporus*. Mol. Gen. Genet. **256**, 179–186
25 Mitchell, A. P. and Magasanik, B. (1983) Purification and properties of glutamine synthetase from *Saccharomyces cerevisiae*. J. Biol. Chem. **258**, 119–124

26 Margelis, S., D'Souza, C., Small, A. J., Hynes, M. J., Adams, T. H. and Davis, M. A. (2001) Role of glutamine synthetase in nitrogen metabolite repression in *Aspergillus nidulans*. J. Bacteriol. **183**, 5826–5833
27 Pesole, G., Bozzetti, M. P., Lanave, C., Preparata, G. and Saccone, C. (1991) Glutamine synthetase gene evolution: a good molecular clock. Proc. Natl. Acad. Sci. U.S.A. **88**, 522–526
28 Barel, I., Bignell, G., Simpson, A. and MacDonald, D. (1988) Isolation of a DNA fragment which complements glutamine synthetase deficient strains of *S. pombe*. Curr. Genet. **13**, 487–494
29 Listrom, C. D., Morizono, H., Rajagopal, B. S., McCann, M. T., Tuchman, M. and Allewell, N. M. (1997) Expression, purification, and characterization of recombinant human glutamine synthetase. Biochem. J. **328**, 159–163
30 Sakakibara, H., Shimizu, H., Hase, T., Yamazaki, Y., Takao, T., Shimonishi, Y. and Sugiyama, T. (1996) Molecular identification and characterization of cytosolic isoforms of glutamine synthetase in maize roots. J. Biol. Chem. **271**, 29561–29568
31 Lea, P. J. (1991) The inhibition of ammonia assimilation: a mechanism of herbicide action. In Herbicides (Baker, N. R. and Percival, M. P., eds.), pp. 267–298, Elsevier, Amsterdam
32 Palacios, R., Blanco, L., Calva, E., Campomanes, M., Chávez, O., Collado, J., López, S., de la Peña, J., Quinto, C. and Sánchez, F. (1980) *Neurospora crassa* glutamine synthetase: a model to study gene expression in eukaryotes. In Glutamine: Metabolism, Enzymology and Regulation (Mora, J. and Palacios, R., eds.), pp. 167–183, Academic Press, New York
33 Calderon, J., Martinez, L. M. and Mora, J. (1990) Isolation and characterization of a *Neurospora crassa* mutant altered in the alpha polypeptide of glutamine synthetase. J. Bacteriol. **172**, 4996–5000
34 Bennett, M. and Cullimore, J. (1990) Expression of three plant glutamine synthetase cDNA in *Escherichia coli*. Formation of catalytically active isoenzymes, and complementation of a glnA mutant. Eur. J. Biochem. **193**, 319–324
35 de la Torre, F., Garcia-Gutierrez, A., Crespillo, R., Canton, F. R., Avila, C. and Canovas, F. M. (2002) Functional expression of two pine glutamine synthetase genes in bacteria reveals that they encode cytosolic holoenzymes with different molecular and catalytic properties. Plant Cell Physiol. **43**, 802–809
36 Grotjohann, N., Kowallik, W., Huang, Y. and Schulte in den Baumen, A. (2000) Investigations into enzymes of nitrogen metabolism of the ectomycorrhizal basidiomycete, *Suillus bovinus*. Z. Naturforsch. (C) **55**, 203–212
37 Muhitch, M. J. (1989) Purification and characterization of two forms of glutamine synthetase from the pedicel region of maize (*Zea mays* L.) kernels. Plant Physiol. **91**, 868–875
38 Kretovich, W. L., Evstigneeva, Z. G., Pushkin, A. V. and Dzhokharidze, T. Z. (1981) Two forms of glutamine synthetase in leaves of *Cucurbita pepo*. Phytochemistry **20**, 625–629
39 Stewart, G. R., Mann, A. F. and Fentem, P. A. (1980) Enzymes of glutamate formation: glutamate dehydrogenase, glutamine synthetase and glutamate synthase. In The Biochemistry of Plants: a Comprehensive Treatise, vol. 5 (Miflin, B. J., ed.), pp. 271–327, Academic Press, New York
40 Mora, J., Dávila, G., Espín, G., González, A., Guzmán, J., Hernández, G., Hummelt, G., Lara, M., Martínez, E., Mora, Y. and Romero, D. (1980) Glutamine metabolism in *Neurospora crassa*. In Glutamine: Metabolism, Enzymology and Regulation (Mora, J. and Palacios, R., eds.), pp. 185–211, Academic Press, New York
41 Finnemann, J. and Schjoerring, J. K. (2000) Post-translational regulation of cytosolic glutamine synthetase by reversible phosphorylation and 14-3-3 protein interaction. Plant J. **24**, 171–181
42 Riedel, J., Tischner, R. and Mack, G. (2001) The chloroplastic glutamine synthetase (GS-2) of tobacco is phosphorylated and associated with 14-3-3 proteins inside the chloroplast. Planta **213**, 396–401
43 Javelle, A., Rodriguez-Pastrana, B. R., Jacob, C., Botton, B., Brun, A., Andre, B., Marini, A. M. and Chalot, M. (2001) Molecular characterization of two ammonium transporters from the ectomycorrhizal fungus *Hebeloma cylindrosporum*. FEBS Lett. **505**, 393–398
44 Javelle, A., Morel, M., Rodriguez-Pastrana, B. R., Botton, B., André, B., Marini, A. M., Brun, A. and Chalot, M. (2003) Molecular characterizaton, function and regulation of ammonium transporters (Amt) and ammonium-metabolizing enzymes (GS, NADP-GDH) in the ectomycorrhizal fungus *Hebeloma cylindrosporum*. Mol. Microbiol. **47**, 411–430
45 Ewaze, J. O., Moore, D. and Stewart, G. R. (1978) Coordinate regulation of enzymes involved in ornithine metabolism and its relation to sporophore morphogenesis in *Coprinus cinereus*. J. Gen. Microbiol. **107**, 343–357
46 Brewin, N. J. (1991) Development of the legume root nodule. Annu. Rev. Cell Biol. **7**, 191–226

Received 22 January 2003/28 March 2003; accepted 8 April 2003
Published as BJ Immediate Publication 8 April 2003, DOI 10.1042/BJ20030152